The Global Circulation Features of the Troposphere between the Equator and 40° N, based on a Single Day's Data

Part 1. The structure of the basic meteorological fields

By FRIEDRICH DEFANT and HENRY M. E. VAN DE BOOGAARD, *Institute of Meteorology, University of Stockholm*

(Manuscript received March 22, 1963)

ABSTRACT

The atmospheric circulation during a single day (December 12, 1957) between the equator and latitude 40° N has been investigated. Using the extensive IGY data the fields of the geopotential height and the two horizontal velocity components have been analyzed for ten isobaric levels and the zonal means of these variables computed. The Hadley circulation cell obtained for this single day agrees quite well with previous mean values computed for a month or a season. The results suggest that the mean circulation in tropical latitudes can be obtained with fair accuracy from analysis of a single day or of a period much shorter than those commonly used.

General

Over the past decade many studies have appeared describing the general circulation features of the atmosphere. Of these may be mentioned J. BJERKNES (1951, 1955), MINTZ (1951), PALMÉN (1955), PISHAROTY (1955), RIEHL and YEH (1950), TUCKER (1959), VUORELA (1957). In most cases these studies were mainly concerned with a period of monthly or seasonal extent covering a latitude range 20° N–70° N and assumed the geostrophic wind relationship to be applicable. In the case of J. BJERKNES (1955) and PISHAROTY (1955) daily variations of specific circulation features were studied using geostrophic assumption. In other cases, e.g. PALMÉN (1955), RIEHL and YEH (1950) and TUCKER (1958), where the investigation of the meridional circulations was the prime object, the actual wind data, available for a number of stations and averaged over a period, were employed.

To date the study of circulation features on global scale of the atmosphere on a daily basis, using the spatially analysed basic meteorological fields, such as the u- and v-components, specific humidity, etc., has not been undertaken. This has mainly been due to the fact that the spatial distribution of observations over many parts of the earth was so poor that no confidence could be attached to the analysis. With the advent of the International Geophysical Year a promising improvement was envisaged. A close investigation into the data position by the authors for the World Meteorological Interval 12–21 December 1957, for which period all available radiosonde, rawind, pilot balloon and other relevant data was plotted for both 00 and 12 GMT (for the pilot balloon 06 GMT also) proved that the available data warranted analysis of the basic fields for the northern hemisphere and that interpretation could confidently be attached to studies on a daily basis of physical properties of the atmosphere such as, meridional momentum, kinetic energy and water-vapour flux. The purpose of the present investigation is therefore to show the feasibility of performing such computations for a single day (12 Dec. 1957) in the manner indicated above, for the latitude belt 0°–40° N.

The investigation has been divided into four parts as follows:

Part 1: The structure of the basic meteorological fields.
Part 2: The angular momentum transport.
Part 3: The kinetic energy transport.
Part 4: The meridional transfer of water vapour.

Parts 1, 2 and 3 are undertaken by the authors jointly and are described in a series of three papers. Part 4 was investigated by the second author and will appear as a separate paper.

Data. As mentioned above the World Meteorological Interval, 12–21 December 1957 was chosen. The choice was random in so far that the world intervals were concentrated periods of intensive observations and that for a start winter data for the belts under consideration was required. In order to obtain a clear insight into the data position all available radiosonde ascents for the entire period and for both 00 and 12 GMT between 40° N and the South Pole were plotted on enlarged thermodynamic diagrams (Rossby-type diagrams University of Chicago, from IM209B). The basic observational data were taken from the "Northern Hemisphere Data Publication, Part 1", U.S. WEATHER BUREAU (1957) and the IGY microcards, WMO (1957). For the Japanese region the excellent publication "Aerological Data of Japan" of the JAPANESE METEOROLOGICAL AGENCY (1957) was taken. On the average a total of 230 radiosonde observations were realized per synoptic time for the latitude belt under consideration.

For each station the meteorological elements, temperature, dewpoint or relative humidity, geopotential height as well as wind direction and speed and u- and v-components were plotted on the thermodynamic diagram to a limited height of 30 mb. The separate rawind reports were used to complete the wind data given in the radiosonde reports. Over the African region south of the Sahara the 06 GMT upper-air reports (06 GMT being the main observation time over this region) were substituted for the 00 GMT data. To supplement the wind data the pilot balloon reports (about 200 per observation time) between 0°–40° N for 00, 06, 12 and 18 GMT were extracted. As these balloons generally reached levels of between 6 and 9 km, an astonishingly good coverage in the windfield was achieved over many regions, e.g. Africa and India.

It must of course be realized that over certain parts, e.g. the central regions of the Eastern Pacific, data are poor and even non-existing. Over other parts, even though data are available, it does not warrant straight-forward u- or v-component analysis. Here, however, by making streamline analyses a more general interpretation to the existing data could be given.

List of symbols. For convenient reference a list of symbols used is given below.

α = radius of earth.
(x,y,z) = cartesian coordinate system. x eastward, y northward and z vertical coordinate in the tangent plane system.
(λ,φ,z) = polar coordinate system. λ eastward, φ northward and z vertically directed.
p = pressure coordinate directed vertically upward and replacing the z-coordinate under the assumption of hydrostatic equilibrium.
u,v,w = respective east, north and vertical wind components.
$\mathbf{i},\mathbf{j},\mathbf{k}$ = unit vector in the east, north and vertical direction respectively.
$\mathbf{v}$ = total wind vector.
ω = vertical velocity in the p-system and equal to the individual derivative of pressure with respect to time (dp/dt).
ϱ = density of dry-air.
Ω = angular velocity of rotation of the earth.
$f = 2\Omega\sin\varphi$ = coriolis parameter.
$\phi = gz$ = geopotential measured in geopotential meters.
g = acceleration of gravity.
$\overline{}$ = baroperator indicating a zonal average of a quantity.
ε' = spatial departure of a quantity ε from $\overline{\varepsilon}$.
L = "effective length" of latitude circle i.e. that part of latitude circle actually occupied by the atmosphere.
M_a = absolute angular momentum.
τ = stress.
K = kinetic energy per unit mass.
K_m = kinetic energy per unit mass of the mean motion.
K_e = kinetic energy per unit mass of the eddy motion.

1. The geopotential field

The first field to be analysed was the geopotential height field. The geopotential height was plotted at each available station and at various pressure surfaces (1000, 900, 850, 700, 600, 500, 400, 300, 200 and 150 mb). The basic charts used were Mercator Projection maps designed by the authors. The scale of the chart was 1:25,000,000 and standard parallel 22½°. The field was analysed at each level and particular care was taken in ensuring vertical continuity. In middle latitudes and up to 700 mb the analysis was performed with a contour spacing of 10 g.p.m., but for the remaining higher levels a spacing of 50 g.p.m. was used. For the tropics 10 g.p.m. spacing was used at all pressure surfaces.

After completion of the analysis, grid values (every five degrees latitude and longitude) were read off, tabulated and latitudinal averages computed. Some testing with a more and less dense gridpoint system was undertaken. It was found that a 72-point grid around a latitude circle was the minimum amount of points that could be used for obtaining a reliable mean value. This is especially true in our case where only a single day's data is taken and where consequently higher wave number disturbances play an important role.

Table 1 gives the numerical values of these latitude averages of the geopotential field at the various pressure surfaces. For the surfaces not analysed the values were interpolated. Fig. 1 gives a graphical representation of this field. Here for each pressure level the vertical distance between two consecutive points gives the averaged height difference for five degree latitude spacing, the value of which can be read

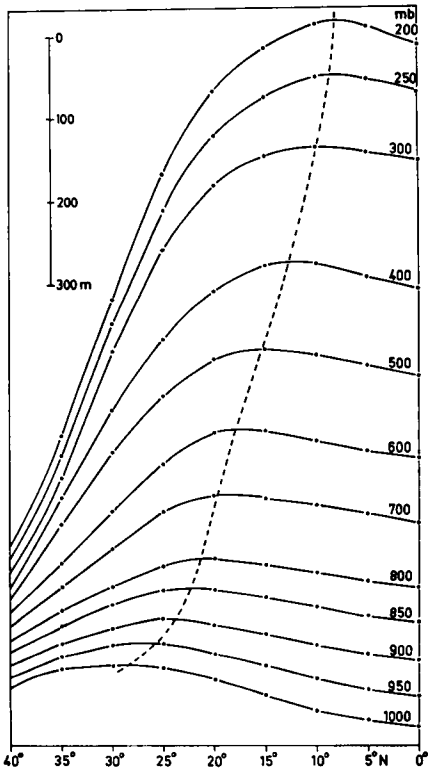

FIG. 1. The variation with latitude of the averaged geopotential height field at various pressure levels. The vertical distance between two consecutive points at a particular level is proportional to the height scale given at the upper right-hand corner.

TABLE 1.

	lat.								
mb	40°	35°	30°	25°	20°	15°	10°	5°	0°
150	13,619	13,761	13,913	14,043	14,129	14,173	14,196	14,193	14,174
200	11,844	11,980	12,142	12,293	12,393	12,445	12,476	12,473	12,450
250	10,356	10,478	10,636	10,778	10,864	10,910	10,935	10,932	10,916
300	9,174	9,305	9,443	9,561	9,643	9,678	9,689	9,684	9,673
400	7,132	7,246	7,343	7,430	7,490	7,522	7,523	7,509	7,490
500	5,581	5,673	5,758	5,824	5,870	5,881	5,875	5,861	5,849
600	4,216	4,270	4,328	4,392	4,430	4,432	4,418	4,407	4,398
700	3,009	3,061	3,100	3,149	3,169	3,166	3,155	3,143	3,135
800	1,953	1,987	2,019	2,043	2,052	2,044	2,035	2,025	2,017
850	1,465	1,495	1,521	1,538	1,540	1,531	1,520	1,508	1,501
900	997	1,025	1,042	1,053	1,048	1,036	1,023	1,011	1,003
950	569	597	609	611	599	585	570	557	548
1000	134	159	161	157	143	124	106	95	86

off on the scale given at the upper right-hand corner of the figure. The dotted line connects the points at each pressure surface where the contour gradient is zero, and where thus the averaged geopotential height field reaches a maximum. This line thus represents the axis of the averaged position of the subtropical anticyclonic belt on this particular day. It is of interest to see how this axis tilts towards the equator with elevation and exists even at high elevations. (At the 1000 mb level at about 29° N and at 200 mb at 7° to 8° N.) To the north of this axis the geopotential height gradient is negative (west wind) and increases sharply with height (increasing west wind with height) and reaches a maximum at 200 mb. At this surface the strongest gradient occurs at about 29° N and corresponds to a geostrophic zonal wind of 37 m/sec. South of the axis the gradient at all levels is positively directed (east wind), but is appreciably weaker. As will be shown later a geostrophic evaluation of the wind at these latitudes give large unrealistic values due to the inaccuracy of the geostrophic assumption in tropical latitudes.

2. The zonal wind field (u-component)

For this field the same method of analysis was used as in the case of the geopotential height field. The values of zonal wind were plotted at the available radiosonde and pilot-balloon stations for the various pressure levels and directly analysed. To make an analysis of this type successfully it is of utmost importance to map the position of the subtropical and polar jet streams. Therefore the authors undertook a special study which ascertained the positions of these jet streams throughout the region. With the aid of this knowledge correct interpretation could be given to strong winds in these regions. For the analysis of the u-field a contour spacing of 5 m/sec was used at all heights. Over the ocean areas where the data was sparse the

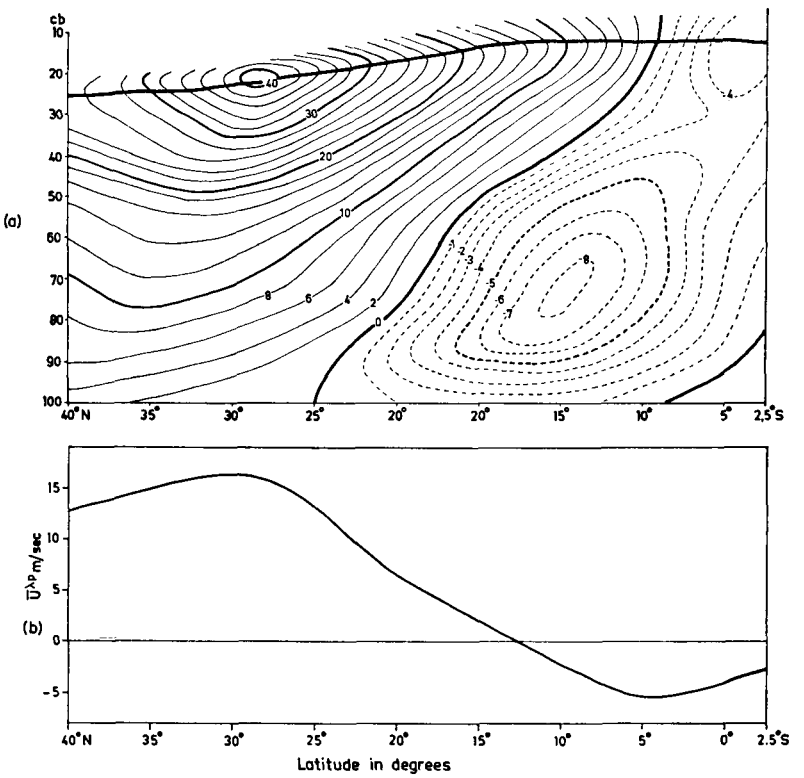

FIG. 2. (*a*) The meridional distribution of the zonal wind component (u) in m/sec. Full lines indicate westerlies dotted lines easterlies. (*b*) Same as (*a*) but integrated with respect to pressure.

geostrophic winds computed from the already available height field, were used north of 15° N to fill these gaps in a most reasonable way. South of this latitude, however, only observed winds were used and analysed as reasonably as possible. Here vertical continuity was considered to be of utmost importance at each latitude.

Fig. 2 gives the meridional distribution of the averaged zonal wind component as a function of pressure. From this picture it is quite apparent that the region under consideration shows the well-known zonal wind distribution with westerlies in its northern and easterlies in its southern half. A slanting zero line situated at 25° N at the surface and sloping equatorward with elevation to about 5° N at 150 mb (about 14 km) separates the two wind regimes. Referring back to Fig. 1 it can be seen that this line closely coincides with axis of the subtropical anticyclonic ridge.

In the regime of zonal westerlies there appears a clearly defined wind maximum at about 29° N and 210 mb elevation. The maximum wind velocity is 41 m/sec. This maximum geostrophic wind computed from Fig. 1 gives 37 m/sec. This value compares well with the winter seasonal average obtained by MINTZ (1951) where the geostrophic maximum wind centre is also situated in about the same position with an intensity of between 40 and 45 m/sec. Attention is drawn to this close agreement and seems to indicate that although large fluctuations will occur from day to day and from place to place along the core of the axis of maximum wind, the daily zonal average value is not likely to differ very much from its seasonal average. This wind maximum is almost entirely due to the quasi-permanent position of the subtropical jet, whilst the strong meandering nature of the polar jet and its generally more northern position is smoothed out by the latitudinal averaging process. An axis of maximum westwind can clearly be noticed and slants somewhat upward from north to south. In this west wind belt the wind increases sharply with elevation until the axis of maximum wind near 200 mb is reached. A sharp decrease occurs again above this layer. Strong wind shears occur also to the north and south of the jet maximum. The easterly regime shows a much weaker intensity than the westerly. Here too a wind maximum can be found; it is situated at about 10° N and between the 800 and 700 mb surface with a core speed of 8 m/sec. This core is the zonal component of the well-known trade-wind belt of the Northern Hemisphere.

MINTZ (l.c.) positions the trade-wind core at approximately the same latitude, but at a much lower elevation. As that part of the meridional wind distribution given by Mintz has mostly been obtained from older climatological tables, the low elevation of the trade-wind core may therefore in his case be questionable. It is, however, of interest to note that the intensity of the trade-wind core obtained in these two studies agrees well. Another notable feature of Fig. 2 is the slope of the axis of maximum easterlies, which between 20° and 15° N is at an elevation of about 900 mb and rises gradually towards the trade-wind core centre. South of this centre the slope of the axis of maximum easterly winds increases rapidly with height. It can further be noted, at e.g. 15° N, that the height and speed of the maximum easterlies agree well with the results obtained by PALMÉN (1955) and VUORELA (1957). There is a strong increase of the easterly winds below the core and a more gradual decrease above. The transition from easterlies to westerlies, however, again show strong vertical wind shear. Since the trade-wind core is more variable in both intensity and position, depending on the time of the year, daily and seasonal average results may differ appreciably. Fig. 2 also gives an indication to a second easterly maximum at higher elevation. This maximum probably indicates the so-called tropical easterly jet, which at this time of the year is generally situated to the south of the equator.

3. The meridional wind field (v-component)

It is well known that direct analysis of the v-component presents many difficulties and different techniques to that used for mapping the u-component had to be resorted to. As a first simple try-out the actual v-components available were averaged latitudinally. Already in this way a surprisingly good indication of the mean meridional circulation (Hadley cell) was obtained between the surface and 400 mb. Above 400 mb the sparsity of the data gave a less clear indication of the upper branch of the

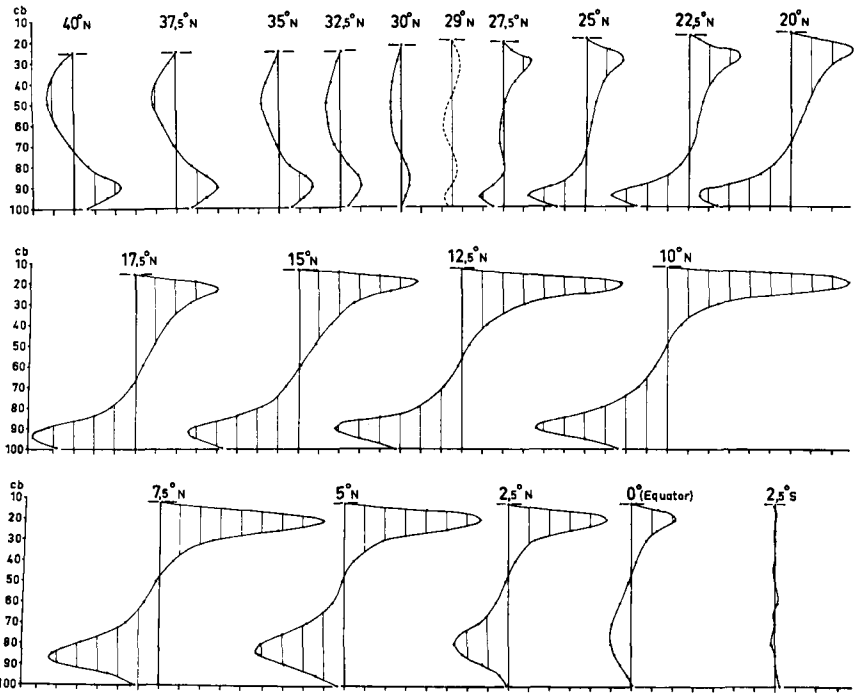

FIG. 3. Vertical profiles of the meridional wind component at different latitudes. The horizontal intervals represent 0.5 m/sec.

Hadley cell directed northward, but there was no doubt about its existence. This preliminary test was encouraging, and paved the way for a more careful computation.

Graphs were prepared with the latitude circle as the horizontal axis. The magnitude of v for all the components at and near the latitude in question was plotted. At the same time the geostrophic meridional wind component was computed for every five degrees longitude and for the latitude in question and results entered on the same graphs. In this way in the regions of good data the relation between the actual and geostrophic value of the meridional wind component could be studied and used to extend the analysis of the actual v-component into regions where no actual wind data was available. This procedure was done for every five degree latitude circle from 40° to 15° N and for all available pressure surfaces. Further south this method failed and actual wind observations had to be relied upon. Special attention was given to the location of the places of vanishing v-component. Vertical cross-sections along each latitude circle and horizontal maps at the various pressure surfaces were constructed. This assured complete horizontal and vertical continuity. Finally, average latitudinal values were obtained at every five degrees latitude and every pressure level.

Fig. 3 gives the vertical profiles of the v-component at each latitude. South of 29° N and up to 2.5° S the direct meridional circulation cell (Hadley) can be clearly seen. The intensity of the cell increases gradually southwards until the maximum speed is reached near 11° N. From there on a decrease occurs until the southern limit of the cell at about 2.5° S. North of 29° N although the v-components are generally much smaller an indication of an indirect circulation cell (Ferrel cell) is apparent.

At this stage the question of vertical mass balance arises. Although mass balances for a single day would not be a stringent requirement, it is obvious that in order to avoid unreasonable pressure changes an almost complete balance should be maintained. The basic question to be answered is where to place the top of the Hadley cell circulation. If the complete vertical field were available, it would be natural to place

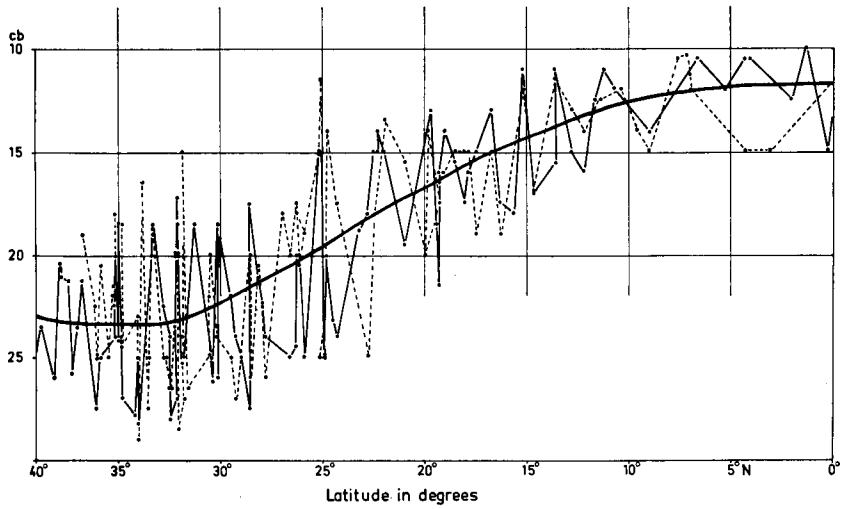

FIG. 4. The height of upper troposphere stability discontinuity as a function of latitude. Full line indicates 00 and dotted line 12 GMT.

the upper limit of the cell where this velocity component vanishes in the upper troposphere. As direct measurements of the vertical velocity cannot be made, other means of finding this level had to be used. As the large-scale vertical velocity component is strongly related to the vertical stability of the atmosphere, an investigation of the vertical stability by means of the available radiosonde ascents was carried out. In earlier investigations FR. DEFANT (1957) has already stated that a sharp change of vertical stability generally occurs in low latitude soundings in the upper troposphere, but still below the tropical tropopause. There the normally existing moist adiabatic lapse rate of the lower troposphere changes abruptly towards a much more stable stratification which finally is terminated by the tropical tropopause at about 16 km elevation. On studying all available radiosondes this characteristic change of lapse rate was clearly found in all soundings, and by plotting this characteristic point for each sounding at the latitude in question Fig. 4 was obtained. Apart from the 0000 Z soundings (full lines), also the 1200 Z soundings were used. Although individual fluctuations occur there is

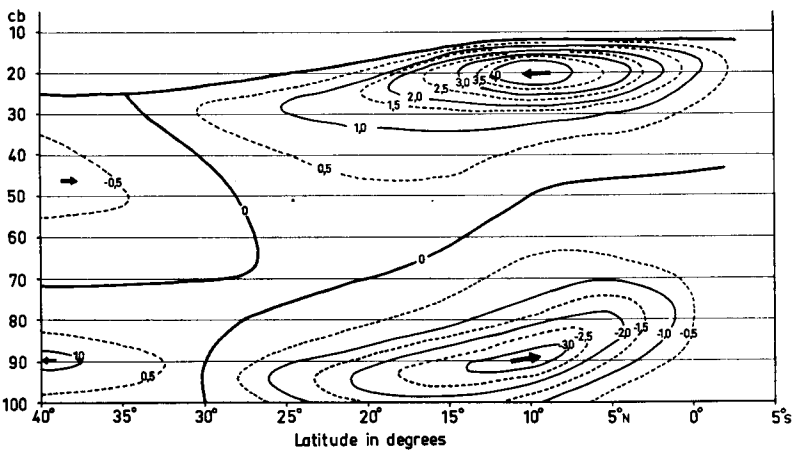

FIG. 5. The meridional distribution of the v-component as a function of pressure.

no doubt that a general dependance on latitude of this characteristic feature exists. The general sense of this dependance is from lower height (250 mb) at higher latitudes to higher elevation (125 mb) near the Equator. It is unlikely that strong vertical velocities connected with the lower tropospheric meridional circulations would exist above this level. This upper limit can also be looked upon as the upper level of cloud penetration and that the atmospheric layer between this level and the tropopause will play a less active role in the tropospheric circulation. From these considerations it was therefore assumed that this line is to be taken as the upper limit of the Hadley cell circulation, where thus the zonally averaged v- and w-components become zero. With these assumptions an almost complete mass balance was obtained for every latitude profile as given in Fig. 3. Only minor changes had to be introduced to obtain an exact mass balance. These were well within the observational error of determination of the v-component.

The meridional distribution of the v-component of the Hadley cell circulation is summarized in Fig. 5. The equatorward branch of the lower tropospheric and the returning poleward branch of the upper troposphere are clearly shown. As in the case of the zonally averaged u-component (see Fig. 2) a gradual equatorward rise of the axis of maximum wind can be observed in the lower branch. Likewise the line of separation of southerly and northerly winds slants in a similar fashion. The maximum core velocity of the southerlies occurring at about 11° N is about 3.5 m/sec.

The centre of the northward branch occurs at about the same latitude, but has an intensity of about 4 m/sec. The intensity of the v-component branch of the Hadley cell obtained here is somewhat stronger than those obtained by PALMÉN, RIEHL and VUORELA (1958), which are, however, seasonal averages.

4. The zonally averaged divergence field and the associated vertical velocity field

With the results obtained so far it is of interest to investigate the zonally averaged field of divergence and from this to compute the zonally averaged vertical velocity field ($\overline{\omega}$).

The zonally averaged continuity equation assuming steady state can be written as follows:

$$\mathrm{div}_H \bar{\mathbf{v}} = \frac{\partial \bar{v}}{\partial y} - \frac{\bar{v}}{a} \mathrm{tg}\, \varphi = -\frac{\partial \overline{\omega}}{\partial p}, \qquad (1)$$

where the meaning of the symbols has been given above. The horizontal bar indicates averaging with respect to latitude. The left-hand side of this equation has been computed from Fig. 5 and the results are given graphically in Fig. 6. Regular fields of vergence are shown with centres of divergence at low elevations in the northern half and at high elevations in the southern half of the meridional plane. Convergence occurs at low elevations in the

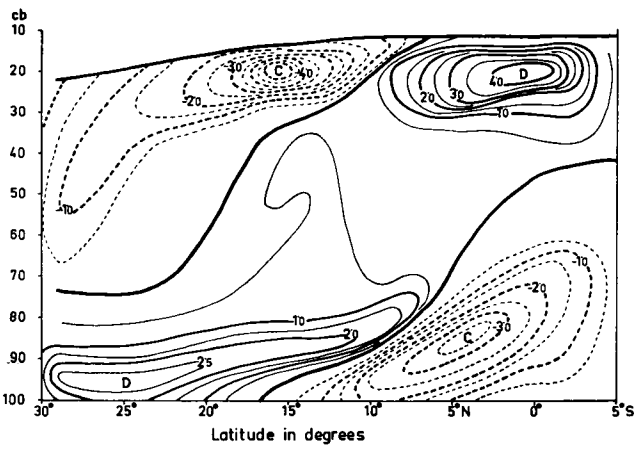

FIG. 6. The distribution of the zonally averaged field of vergence in a meridional plane. Full lines = divergence, dotted lines = convergence.

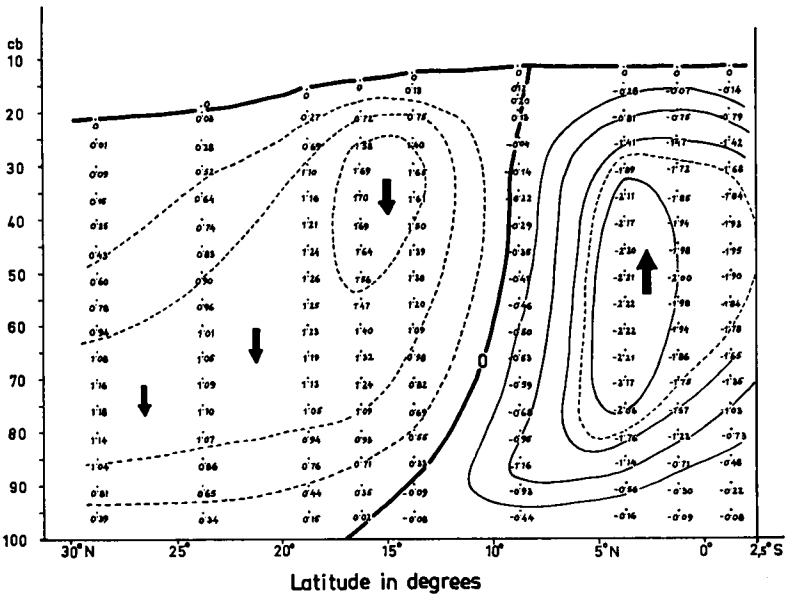

FIG. 7. The meridional distribution of the zonally averaged vertical velocity component $\overline{\omega}$. Full lines denote upward, dotted lines downward motion. Values are given in mb/hour.

southern half and at high elevations in the northern half of the meridional plane. Thus larger values of vergence are confined to layers near the ground and to layers close to the upper boundary. The space in the mid-troposphere can be considered as a deep layer of almost zero vergence. By integrating equation (1) with respect to pressure the $\overline{\omega}$-field is readily obtained and is represented in Fig. 7. Narrow and relatively intense upward motions in low latitudes with maximum values of about 2 mb/hour (about 1.1 m/sec) exist in the mid-tropospheric part between 10° N and 2½° S. Sinking motion is observed in the northern half of the cell inside a broader latitudinal belt between 10° N and 29° N showing maximum values of 1.7 mb/hour (about 0.9 m/sec). In the case of the belt of upward motion the axis of max. vertical velocities is orientated almost vertically, whilst in the region of descent this axis slopes strongly.

5. The Mass Transport of the Hadley Cell

With the fields of zonally averaged v- and ω-components available it is now possible to compute the mass-transport associated with the Hadley cell. For a given pressure interval p_1 to p_2 the meridional mass transport (m_φ) can be given:

$$[m_\varphi]_{p_1}^{p_2} = \frac{2\pi a \cos\varphi}{g} \int_{p_2}^{p_1} \bar{v}\, dp. \qquad (2)$$

A computation of this meridional mass-transport was performed at each five degrees latitude interval for layers of 10 cb in vertical extent. The corresponding vertical mass-transport between two latitude circles φ_1 and φ_2 is given by:

$$[m_p]_{\varphi_1}^{\varphi_2} \cong -\frac{2\pi a^2}{g} \int_{\varphi_1}^{\varphi_2} (\overline{\omega} \cos\varphi)\, d\varphi. \qquad (3)$$

This formula was, however, not used because due to the assumption of a steady state the necessary vertical mass transport may be obtained from the meridional mass-transport assuming zero vertical transport at the lower and upper limit of the cell. Fig. 8 gives a graphical representation of the result. The larger numbers give the magnitude of the meridional-transport (m_φ) in units of million tons/sec. The upper northward branch as well as the lower southward branch of the meridional circulation are well reflected by the isolines of equal mass-transport (heavy full and dotted lines). The smaller numbers in between give the vertical mass-transport (m_φ) necessary to obtain a steady state. An equal amount of mass is carried upward and downward at each individual

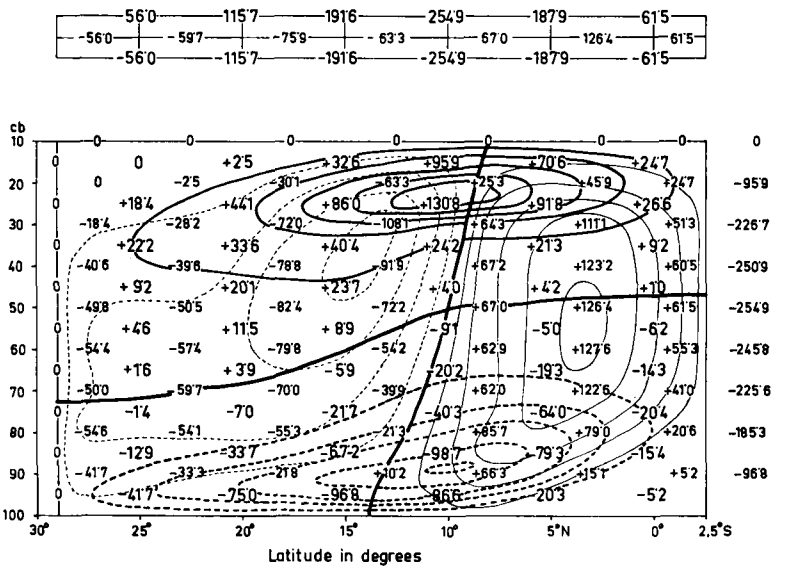

FIG. 8. The horizontal and vertical mass transport of the Hadley cell in units of million tons per second.

pressure level and is shown by the figures to the right. The small table at the top of Fig. 8 shows integrated mass-transport for the different branches of the Hadley cell. From this it can be seen that the total mass circulation in the Hadley cell amounts to 255 million tons/sec, a figure which agrees very well with 260 million tons/sec obtained by PALMÉN, RIEHL and VUORELA (1958). Again it is noteworthy that the mass-transport obtained for a single day so closely agrees to seasonal average figures. The computational results of about 90 million tons/sec obtained by MINTZ (1955*a*) seems then to be a severe underestimate, a fact pointed out by PALMÉN (1955).

REFERENCES

BJERKNES, J., 1951, *The maintenance of the zonal circulation of the atmosphere.* P. V. Meteor. Un. geod. geophys. int., Brussels I–XXIII. (Presidential address.)

DEFANT, FR., 1959, *Investigations on the detailed structure of the atmosphere in the Northern Hemisphere mid-summer.* Int. Inst. of Meteor. Stockholm, Rep. to the Brussels Office GRD (Contract AF61(514)–963).

MINTZ, Y., 1951, The geostrophic poleward flux of angular momentum in the month of January 1949. *Tellus*, **3**, pp. 195–200.

MINTZ, Y., 1955, *Final computation of the mean geostrophic poleward flux of angular momentum and of sensible heat in the winter and summer of* **1949**. Dept. Meteor. Univ. Calif., Final Report Gnrl. Circ. Proj., Pap. No. 5 (Contract AF19(122)–48).

MINTZ, Y., and LANG, J., 1955, *A model of the mean meridional circulation.* Dept. Meteor. Univ. Calif., Gnrl. Circ. Proj. Pap. No. 6 (Contract AF19(122)–48).

PALMÉN, E., 1955, On the mean meridional circulation in low latitudes of the Northern Hemisphere in winter and the associated meridional and vertical flux of angular momentum. *Soc. Scien. Fenn. Comm. Phys.-Math., XVII*, 8, pp. 1–33.

PALMÉN, E., RIEHL, H., and VUORELA, L., 1957/58, *On the meridional circulation and the release of kinetic energy in the tropics.* Univ. Chicago, Dept. Meteor. Proj. No. 082–120, Office of Naval Research; and *J. Meteor.*, Vol. **15**, No. 3, pp. 271–277.

PISHAROTY, P. R., 1954, *The kinetic energy of the atmosphere.* Dept. Meteor. Univ. Calif., Gnrl. Circ. Proj., Pap. No. 6 (Contract AF19(122)–48).

RIEHL, H., and YEH, T. C., 1950, The intensity of the net meridional circulation. *Quart. J. R. Met. Soc.*, **76**, pp. 182–188.

STARR, V. P., and WHITE, R. M., 1952, Meridional flux of angular momentum in the tropics. *Tellus*, **4**, pp. 118–125.

TUCKER, G. B., 1959, Mean meridional circulation in the atmosphere. *Quart. J. R. Met. Soc.*, **85**, pp. 209–224.

VUORELA, L., 1957, On the observed zonal and meridional circulations at latitudes 15° and 30° N in winter. *Geophysica*, **6**, No. 2, pp. 106–120.